Supplementary Information for

Piezo1-mediated mechano-energetics regulate CAR T cell function

This Supplementary Information file includes:

Supplementary Methods

Supplementary Figures 1-7

Supplementary Table 1-3

I. Supplementary Methods.

Piezo1 modulation by plasmid transfection and lentivirus transduction

Piezo1 loss-of-function (Piezo1 LOF) and gain-of-function (Piezo1 GOF) studies were achieved via Piezo1 knockout by plasmid transfection and Piezo1 activation by lentiviral transduction. T cells were seeded at a density of 0.5×10^6 cells per well in 24-well plates and subjected to either Piezo1 knockout by PIEZO1 CRISPR/Cas9 KO Plasmid or Piezo1 activation by lentiviral transduction with PIEZO1 Lentiviral Activation Particles. For knockout, cells were transfected with 3 μg of Piezo1 CRISPR/Cas9 plasmid (CAT# sc-410555, Santa Cruz Biotechnology) using UltraCruz® transfection reagent (CAT# sc-395739, Santa Cruz Biotechnology) and Plasmid Transfection Medium (CAT# sc-108062, Santa Cruz Biotechnology). For activation, T cells were transduced with Piezo1 lentiviral particles in the presence of Polybrene (5 μg/mL, CAT# sc-134220, Santa Cruz Biotechnology). To image live-Piezo1, CAR T cells were seeded at a density of 0.5×10^6 cells per well in 24-well plates and transfected with a custom plasmid using Viafect Transfection reagent (CAT#E4981, Promega). The plasmid contains human PIEZO1 coding sequence, split into N- and C-terminal fragments with an EGFP reporter fused internally (VectorID: VB221213-1527ewt, VectorBuilder). In all cases, cultures were refreshed at 48 h with ImmunoCult-XF T Cell Expansion Medium (CAT# 10981, StemCell Technologies) supplemented with recombinant human IL-2 (200 IU/mL, CAT# 200-02, Peprotech) and maintained at 37 °C with 5% CO_2. Successful transfection and transduction were confirmed by immunostaining of Piezo1 or percentage of GFP-expressing cells.

II. Supplementary Figures

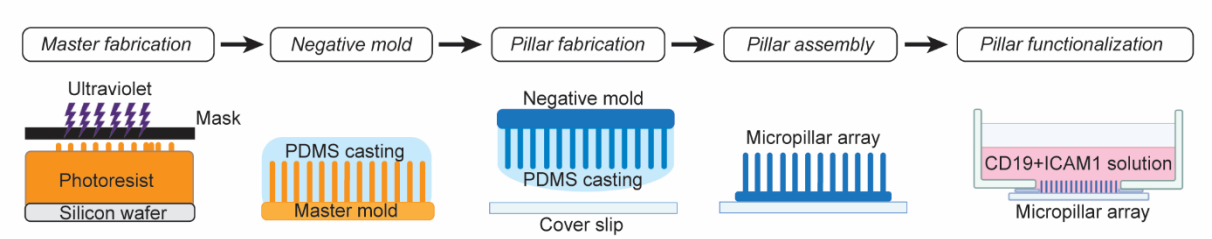

Supplementary Figure 1. **Micropillar array fabrication and functionalization**. Schematic illustration of procedures for PDMS micropillar array fabrication and functionalization. The PDMS micropillar array was fabricated from a double-molding soft lithography process: silicon master mold manufactured using photolithography, PDMS casting of master mold to produce negative mold, and replicating PDMS micropillar array on a glass coverslip from the negative mold. The fabricated micropillar array on glass coverslip was assembled to the bottom of a 35 mm confocal dish, then was functionalized via immersion in a protein solution comprising ICAM-1 and FTIC-conjugated CD19.

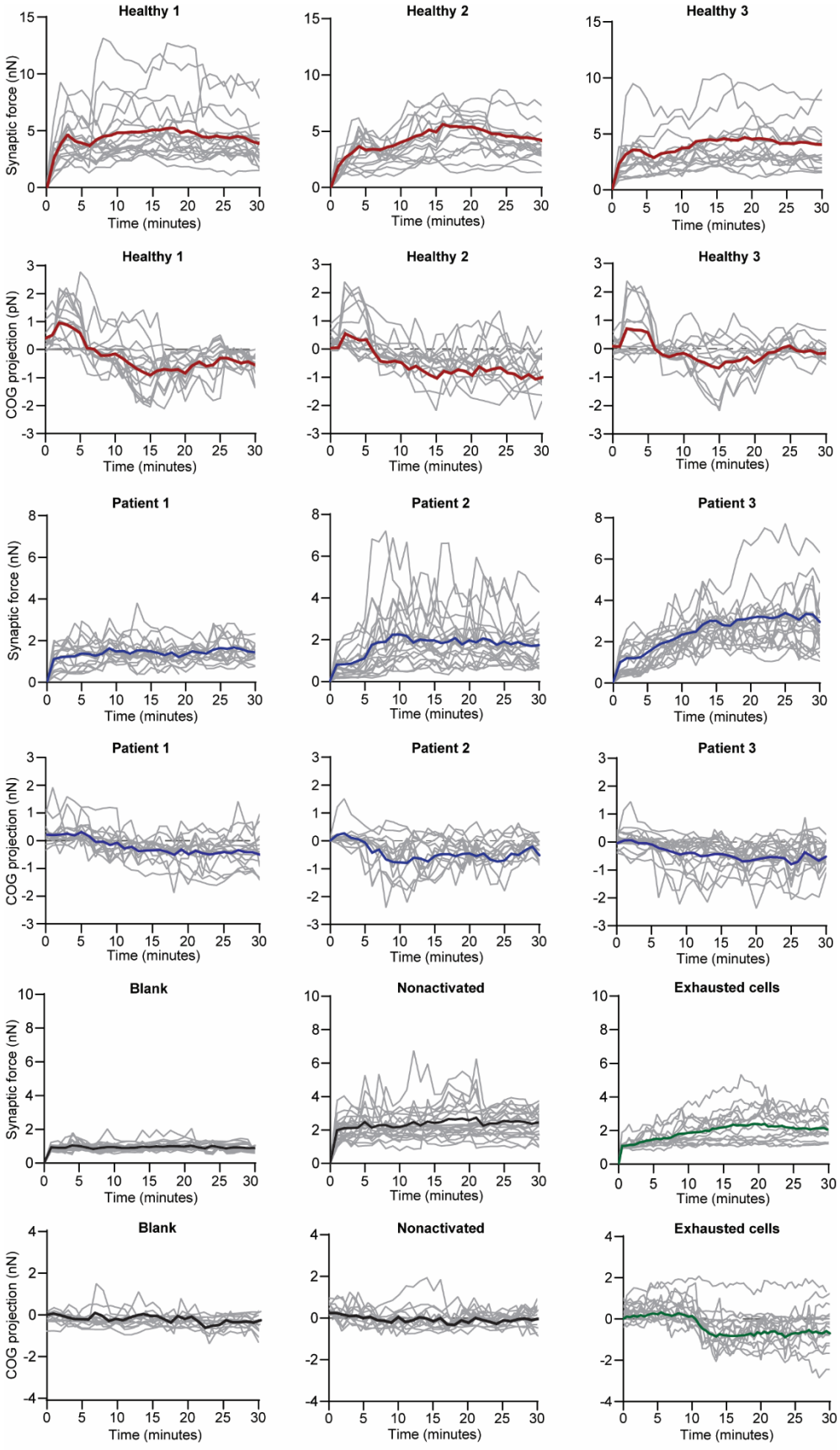
Healthy 1
Healthy 2
Healthy 3
Synaptic force (nN)
COG projection (pN)
Time (minutes)
Patient 1
Patient 2
Patient 3
COG projection (nN)
Blank
Nonactivated
Exhausted cells

Supplementary Figure 2. Mapping the synaptic force dynamics of CAR T cells derived from individual healthy donors, patients, induced exhaustion, and nonactivated cells. Activated CAR T cells derived from healthy donors, patients, and the induced exhaustion group were seeded onto micropillar substrates functionalized with CD19 and ICAM-1. Nonactivated CAR T cells were seeded onto substrates coated with ICAM-1 only, and the blank group was seeded on Poly-L-lysine-coated substrates to assess nonspecific attachment. Grey lines represent force measurements from individual cells; thick colored lines indicate group averages (n = 20 cells per group). All data were obtained from three independent experiments.

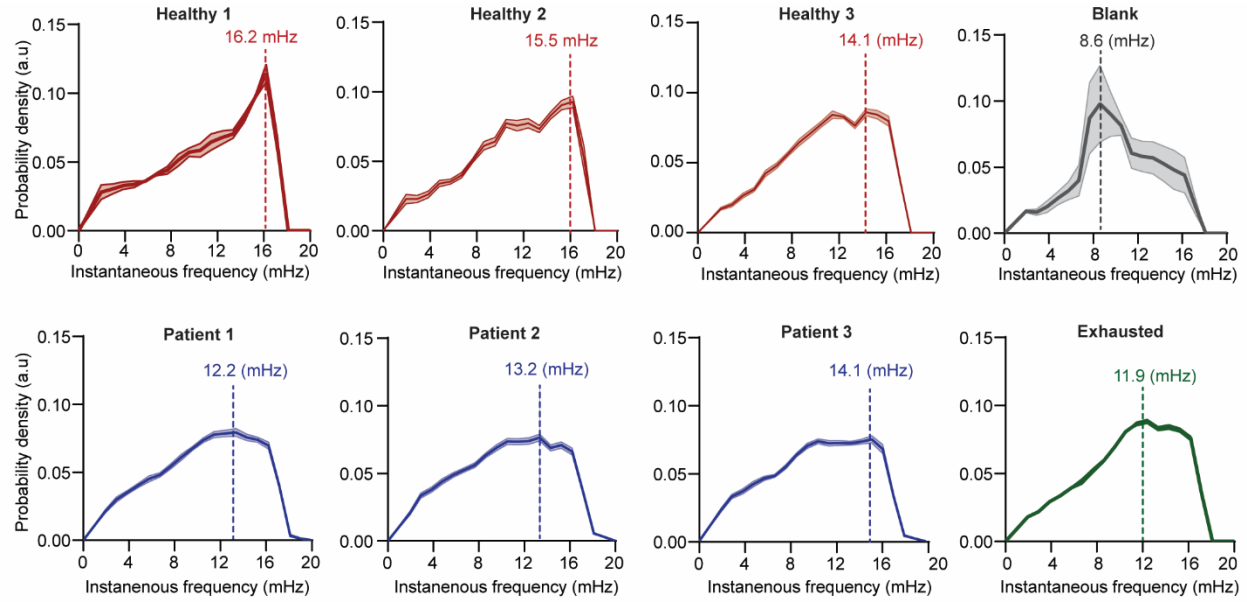

Supplementary Figure 3. Instantaneous frequency spectrum analysis of CAR T cell synaptic force dynamics. The frequency spectrum (n = 20 cells) was calculated from the synaptic force dynamics profiles in Supplementary Figure 2, including CAR T cells derived from individual healthy donors and patients, and exhausted CAR T cells activated on CD19/ICAM-1-functioned PDMS micropillar array, as well as control group of CAR T cells seeded on Poly-L-lysine-coated micropillar array substrates (blank). Thick lines denote mean, shaded areas denote s.e.m. All data was collected from three independent experiments.

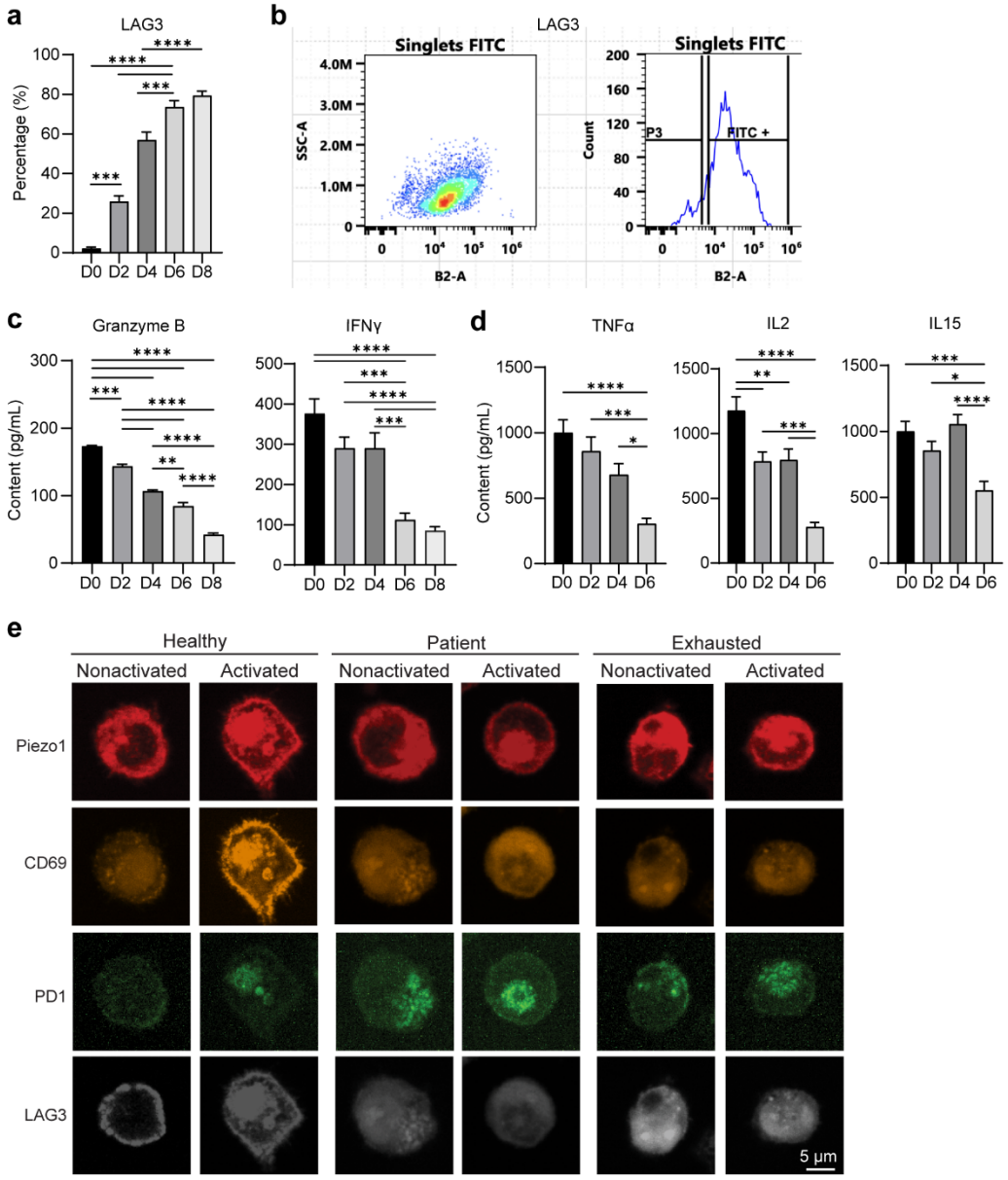

Supplementary Figure 4. Validation of CAR T cell exhaustion phenotypes during serial re-stimulation. (**a**) Flow cytometry results showing percentage of CAR T cells expressing exhaustion marker LAG-3 during an 8 day-period of induced exhaustion in vitro (n = 10). CAR T cells were activated with CD19-coated beads on D0 and re-stimulated by CD19-coated beads every two days. (**b**) Representative images showing gating strategy for flow cytometry analysis for identifying negative and positive cell percentage in healthy CAR T cells stained with LAG-3. All events were first gated on singles by plotting SSC-A against the fluorescence parameter to exclude doublets and aggregates. Within the singlet population, marker-specific gates were then applied. Alexa Fluor 488-tagged LAG-3 positive cells as those falling outside of gate P3 on the B2-A histogram. Positive selection thresholds were established relative to unstained controls to ensure accurate discrimination between positive and negative populations. (**c**) ELISA measured Granzyme B (n=3 technical replicates) and IFNγ (n =10 technical replicates) secretion from CAR T cells over time during induced exhaustion. (**d**) ELISA measured secretion of TNFα, IL2 and IL15 over time during

induced exhaustion (n=10 technical replicates). Data are presented as mean ± s.e.m. Statistical comparisons were performed using one-way ANOVA with Tukey's post hoc test. (**e**) Representative immunostaining images of Piezo1, activation marker CD69, and exhausted markers PD1 and LAG3 in healthy donor-derived, patient-derived and exhausted CAR T cells.

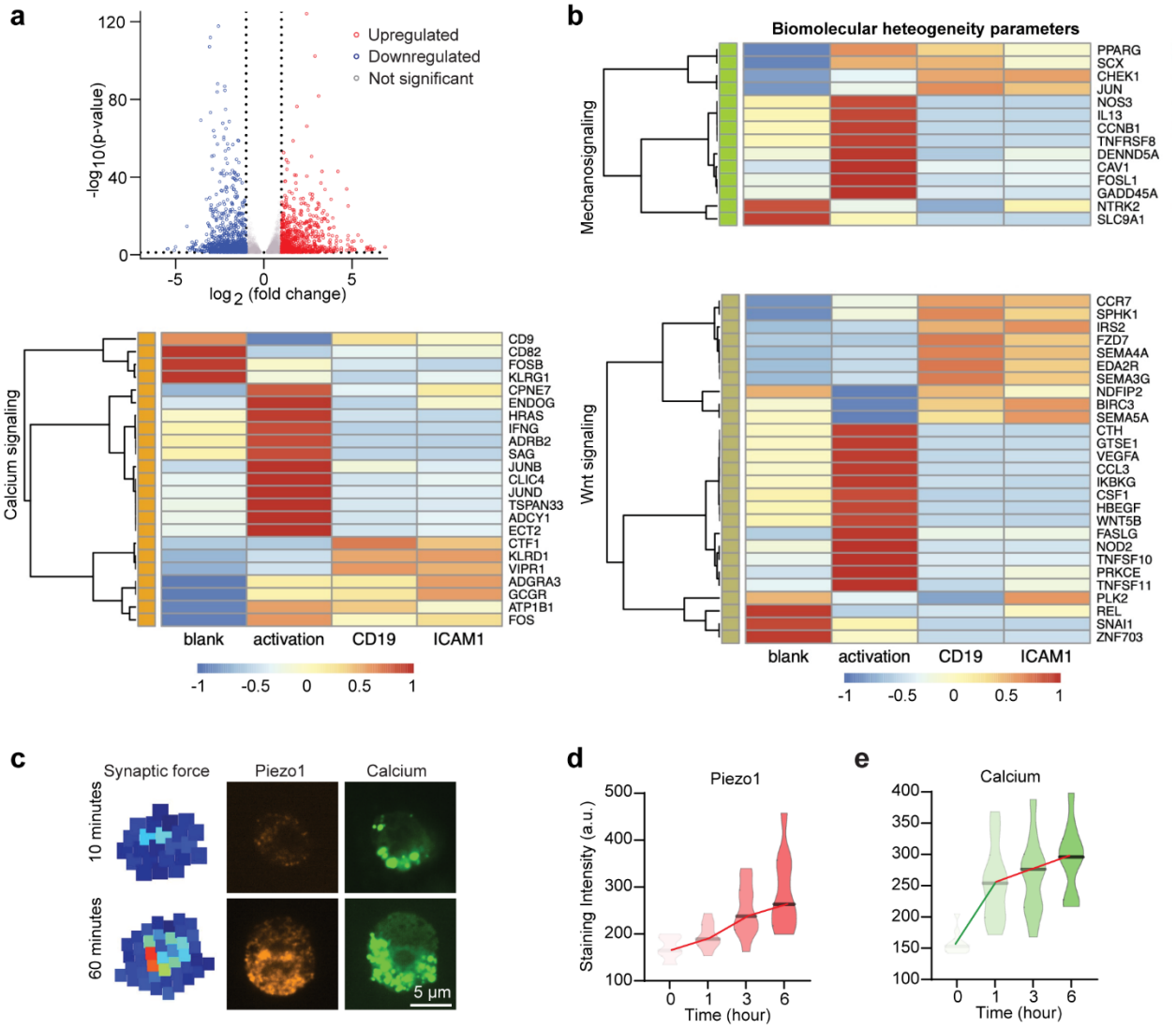

Supplementary Figure 5. Whole-transcriptome analysis with total RNA sequencing of mechanosensitive signaling involved in CAR T cell activation. (**a**) Volcano plot showing differentially expressed genes (DEGs) determined by bulk RNA sequencing using DESeq2 analysis (adjusted $p<0.05$). (**b**) Heatmaps of normalized expression for genes in mechanosignaling, calcium, and Wnt pathways in CAR T cells across four substrates conditions: blank, CD19/ICAM-1 (activation), CD19-only, and ICAM-1-only. Expression values are normalized and genes are hierarchically clustered to highlight co-expression modules. Data was collected from 2 technical replicates per condition. (**c**) Representative synaptic force heatmap, and live imaging of Piezo1 and Ca^{2+} activities measured by Fluo4-AM in CAR T cells 10 and 60 minutes after seeding on CD19/ICAM-1 functionalized micropillar array substrates, showing increase in Piezo1-mediated Ca^{2+} signaling and synaptic force upon activation. (**d**) Quantification of Piezo1 expression and (**e**) intracellular Ca^{2+} activities in CAR T cell upon activation (n = 10 cells). The thick line represents the mean over time and the filled area represents the error bar presented as s.e.m.

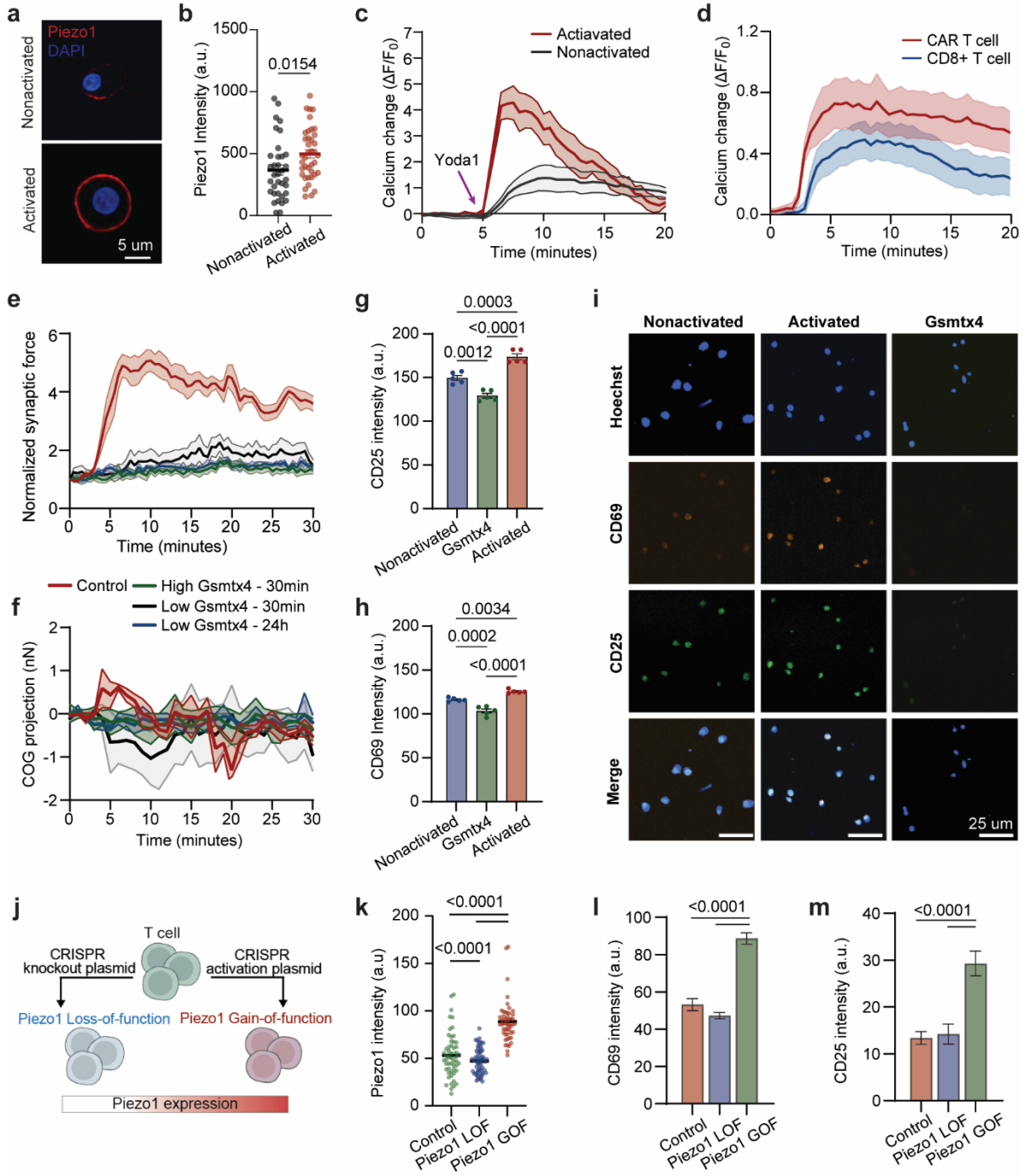

Supplementary Figure 6. Piezo1 regulates force generation and activation of CD8⁺ cytotoxic T cells. (**a**) Representative immunofluorescent images and (**b**) quantification of Piezo1 expression intensity in nonactivated (n = 35 cells) and activated (n = 39 cells) CD8⁺ T cells. Activated T cells were seeded on micropillars functionalized with ICAM-1 (20 μg/mL) and anti-CD3ε/CD28 antibodies (30 μg/mL), while nonactivated controls were seeded on ICAM-1 only. Statistical comparison by two-tailed unpaired Student's t-test. (**c**) Time-course of calcium influx in nonactivated and activated T cells measured using Fluo-4AM (n = 20 cells, 3 independent experiments). Activated T cell group was seeded on glass substrate functionalized with ICAM-1 and anti-CD3ε/CD28 antibodies, while nonactivated group was seeded on glass substrate with

ICAM-1 only. (**d**) Time-course of calcium influx in CD19-activated CAR T cells vs CD3ε/CD28-activated $CD8^+$ T cells measured using Fluo-4AM (n = 20 cells, 2 independent experiments). In c-d, calcium intensity ($\Delta F/F_0$) was normalized to baseline (T = 0 min). (**e**) Normalized synaptic force dynamics and (**f**) force directionality of $CD8^+$ cytotoxic T cells interacting with ICAM-1/anti-CD3ε/CD28-coated micropillars (activated group) or ICAM-1-coated micropillars (nonactivated control group). T cells were pretreated with high-dose (2.5 μM, 30 minutes) or low-dose (1 μM, 30 minutes or 24 hours) GsMTx4, or left untreated (n = 10 cells each group, 2 independent experiments). Data in e, f were normalized to their respective initial values at T = 0 min. (**g-h**) Quantification and (**i**) representative immunofluorescent images of T cell activation markers CD69 and CD25 expression in $CD8^+$ T cells exposed to ICAM-1/anti-CD3ε/CD28-coated substrates (activated) or ICAM-1-only substrates (nonactivated) after 24 hours (n = 5 technical replicates). T cells in GsMTx4 group were pretreated with 2.5 μM GsMTx4 for 30 minutes and exposed to ICAM-1/anti-CD3ε/CD28-coated substrates after 24 hours (n = 5 technical replicates). (**j**) Schematic of Piezo1 modulation via PIEZO1 CRISPR/Cas9 KO Plasmid loss-of-function (Piezo1 LOF) and PIEZO1 lentiviral-based gain-of-function (Piezo1 GOF) constructs. Schematic was created in BioRender. Details see Supplementary Methods. (**k**) Immunofluorescent quantification of Piezo1 expression in control, Piezo1 LOF, and Piezo1 GOF T cells (n = 35 cells). (**l, m**) Expression of CD69 (**l**) and CD25 (**m**) across control (n = 64 cells), Piezo1 LOF (n = 53 cells for CD69, 48 for CD25), and Piezo1 GOF (n = 50 cells for both) groups. In c–f, thick lines denote group means and shaded regions indicate and s.e.m. In g, h, k–m, data are presented as mean ± s.e.m. and p-values were calculated using one-way ANOVA with Tukey's post hoc test.

III. Supplementary Tables

Supplementary Table 1. Summary data for correlation matrix in Figure 1K.

	E_{fe}	CD69	CD25	IFNγ	TNFα	ATP
Activated	7.7684908	254.93325	200.23075	35.99103758	25.58019231	1
Nonactivated	2.2279598	136.61995	134.6762	1.14591623	1.14591623	0.5392367
Patient	4.4988748	168.360687	128.150687	1.009515548	1.429180892	0.3176778

Supplementary Table 2. List of antibodies used in immunofluorescent (IF) and Flow cytometry (Flow) analyses.

Antibody	Vendor and Catalog number	Assay	Dilution
Biotinylated monoclonal anti-FMC63 scFv (CAR)	CAT#FM3-BY54, ACRO Biosystems	IF	1:50
Alexa Fluor 532 anti-CD25	CAT#310916, Thermo Fisher Scientific	IF	1:50
Alexa Fluor 488 anti-CD69	CAT#58-0251-82, Thermo Fisher Scientific	IF	1:50
PE-conjugated anti-CD69	CAT#310906, clone BL-CD6, BioLegend	Flow	1:30
PE-conjugated anti-CD25	CAT#302606, clone BC96, BioLegend	Flow	1:30
PE anti-human CD279 (PD-1)	CAT#329906, BioLegend	IF	1:30
FITC anti-human CD223 (LAG-3)	CAT#369308, BioLegend	IF, Flow	1:50
FITC anti-human CD54	CAT#322720, BioLegend	IF	1:50
Alexa Fluor 555 Phalloidin	CAT#A34055, Thermo Fisher Scientific	IF	1:300
Piezo1 monoclonal antibody	CAT#MA5-32876, Thermo Fisher Scientific	IF	1:200
Alexa Fluor 488 Piezo1 Antibody	CAT#NBP1-78446AF488, Novus Biologicals	Digital ELISA	1:100
Pacific BlueTM anti-human CD69	CAT#310919, Biolegend	Digital ELISA	1:100
FITC anti-human CD31	CAT#303104, BioLegend	IF	1:50
APC anti-human CD90	CAT#328113, BioLegend	IF	1:50
Alexa Fluor 488 anti-Ki-67	CAT#151204, BioLegend	IF	1:50
LIVE/DEAD fixable aqua dead cell stain Kit	CAT#L34965, Thermo Fisher Scientific	Flow	1:200
APC-goat anti-mouse secondary antibody	CAT#A-865, Invitrogen	IF	1:400
DAPI	CAT#D3571, Invitrogen	IF	1:1000
Hoechst 33342	CAT# H3570, Invitrogen	IF	1:1000

Supplementary Table 3. The primer sequences used qRT-PCR analysis.

Gene	Forward sequence	Reverse sequence
PIEZO1	CCTGGAGAAGACTGACGGCTAC	ATGCTCCTTGGATGGTGAGTCC
PIEZO2	GACGGACACAACTTTGAGCCTG	CTGGCTTTGTTGGGCACTCATTG
TRPV4	TCACTCTCACCGCCTACTACCA	CCCAGTGAAGAGCGTAATGACC
ORAI1	AGGTGATGAGCCTCAACGAGCA	AGTCGTGGTCAGCGTCCAGCT
STIM1	CACTCTTTGGCACCTTCCACGT	CTGTCACCTCGCTCAGTGCTTG
AKT1	TGGACTACCTGCACTCGGAGAA	GTGCCGCAAAAGGTCTTCATGG
mTOR	AGCATCGGATGCTTAGGAGTGG	CAGCCAGTCATCTTTGGAGACC
YAP	TGTCCCAGATGAACGTCACAGC	TGGTGGCTGTTTCACTGGAGCA
ITPR3	GCAACCACATCTGGACGCTCTT	AGAAGGCGTTGATGGTGTCCAG
NFAT1	GATAGTGGGCAACACCAAAGTCC	TCTCGCCTTTCCGCAGCTCAAT
WASF1	CCCTACCTGTAATCAGTGATGCC	GCTTCCTGTTCACGCTGCTCTT
CAMK2A	GAGCCATTCTCACCACGATGCT	TGGTGTTGGTGCTCTCTGAGGA
MST1	CCACATCAGCACCGATTTACGC	CGTCGAGGTTCCAGCAGAAGTT
MST2	GGCAGATTTTGGAGTGGCTGGT	AATGCCAAGGGACCAGATGTCG
TRPC1	CCAAACTGCTGGTGGCAATGCT	GGAATGATGTTGAAAGGTGGAGG
TRPM7	GAAGCACCATCTTGGACTCTTGC	GGACCACAGATTTGAGGGATAAC